

Optimal Biopsy Protocols for Prostate Cancer

Ariela Sofer¹, Jianchao Zeng², Brett Opell³, John J. Bauer⁴, and Seong K. Mun²

Abstract

Prostate cancer is the second leading cause of cancer-related death among American men. Biopsy for prostate cancer is a procedure known as transrectal ultrasound-guided needle biopsy. Because of the low resolution of ultrasound, the urologist cannot usually distinguish between cancerous and healthy tissue. For this reason, most biopsies follow standard protocols based on long-term experience of physicians. Recent studies indicate that these protocols have a significant rate of false negative diagnoses. In this research we use real prostate specimens removed by prostatectomy to develop a 3-D distribution map of cancer in the prostate, and use this to develop optimized biopsy procedures. The new procedures have the potential to increase the rate of early detection of prostate cancer, and thus decrease the rate of mortality.

1. Introduction

Prostate cancer is the most diagnosed form of cancer, other than skin cancer, in the United States. It is the second leading cause of cancer-related death among men, exceeded only by lung cancer. The American Cancer Society estimates that about 180,400 new cases of prostate cancer will be diagnosed in 2000, and that approximately 32,000 men will die of the disease. Prostate cancer is therefore a serious public health concern.

Early screening for prostate cancer is usually done by digital rectal examination, and by measurement of the level of the patient's prostate specific antigen (PSA) - a protein made by prostate cells. Patients with prostate cancer often have elevated levels of PSA. However elevated PSA levels may be indications of other conditions, such as *prostatic hyperplasia* (noncancerous prostate enlargement) and *prostatitis* (inflammation of the prostate), and some healthy men naturally have elevated levels of PSA. Men with high PSA results are advised to have a biopsy to determine whether indeed they have cancer.

The biopsy procedure for prostate cancer is known as transrectal ultrasound-guided (TRUS) needle biopsy. Using ultrasound guidance the urologist inserts a needle through the wall of the rectum into the prostate, and removes a cylinder of tissue. The number of needle samples may vary between three or four, to as many as eighteen. The number of needles to be used and their location in the prostate is termed the *biopsy protocol*.

TRUS guided needle biopsy, is, as its name suggests, an uncomfortable procedure. Consequently, a patient's first biopsy usually involves a small number of needle samples. Due to the low resolution of ultrasound, the urologist cannot usually distinguish normal prostate

¹Department of Systems Engineering and Operations Research, George Mason University

²Imaging Science and Informations Systems Center, Department of Radiology, Georgetown University Medical Center

³Urology Division, Department of Surgery, Georgetown University Medical Center

⁴Urology Service, Walter Reed Army Medical Center

tissue from cancerous tissue during the biopsy. For this reason, a number of standard biopsy protocols have been developed, to assist the urologist in performing the biopsy.

The biopsy protocol most commonly used is the systematic sextant biopsy [Hodge et al. 1989]. Recent studies [Bankhead 1997, Rabbani et al., 1998] have shown, however, that this strategy has an unacceptable level of false negative diagnoses (about 20%), and that many patients who have a negative initial biopsy are found to have cancer in repeat biopsies. The article by O'Dowd, et al. [O'Dowd 2000] concludes that the initial biopsy strategy needs to be improved and/or expanded to increase the overall cancer detection rate.

Recent clinical studies have investigated new protocols that have improved detection rates. Eskew et al. [1997] investigated a 5-region biopsy protocol in which additional lateral and midline biopsies were added systematically to the traditional sextant biopsy. On a study group of 48 patients with cancer, the protocol was superior to the sextant method in detecting cancer. In a test on 121 cancer patients, Chang et al. [1997] found that adding 4 lateral peripheral biopsies to the sextant method increased the number of detected cancers from 99 to 116. Bauer, Zeng et al. [1999] have also showed that biopsy protocols that add laterally placed needles to the traditional sextant are superior to the sextant method.

The goal of our research is to develop optimized biopsy protocols. For a specified number of needles, an optimal protocol is one that maximizes the probability of detection of cancer in a patient. A major component of our effort is the development of a statistical distribution map of cancer in the prostate.

The map is constructed from cancerous prostates that were removed via prostatectomy. Each of the prostates is first reconstructed into a 3-D computerized model that accurately represent the anatomy of the prostate, and the distribution of cancer within it. Next, each model is divided into zones based on clinical conventions, and the presence of cancer in each zone is calculated. From this the 3-D distribution map of tumor location is developed. Two hundred and eighty one prostates have been reconstructed and analyzed thus far.

The paper is organized as follows. Section 2 gives a brief discussion of the 3-D computer reconstruction of prostate specimens, and Section 3 describes how the cancer distribution map is created. Section 4 presents the optimization models that define the optimal protocols, followed by a discussion of the optimal biopsy protocols in Section 5. Conclusions are given in Section 6.

2. 3-D Computer Reconstruction of Prostate Specimens

The reconstruction of the prostates involved several steps. Each prostate was sectioned in $4\mu\text{m}$ sections at 2.25mm intervals, and each slice was digitized with a scanning resolution of 1500 dots per inch. Each digitized image was segmented by a single pathologist to identify the key pathological structures, including surgical margins, capsule, urethra, seminal vesicle, and the tumor. The contours of each structure were identified on each slice, and then stacked up. Interpolation between pairs of contours was performed using a 3-D elastic contour model. The 3-D model of each structure in the prostate was finalized by tiling triangular patches onto the interpolated contours, using a deformable surface-spine model, that employs a second-order partial differential equation to control the deformation of the surface. The reconstruction technique is described in detail in [Zeng et al.,1998a]. The successive steps of the reconstruction are illustrated in Figure 1.

The computer reconstructions have also been used [Zeng et al, 1998b] in the development

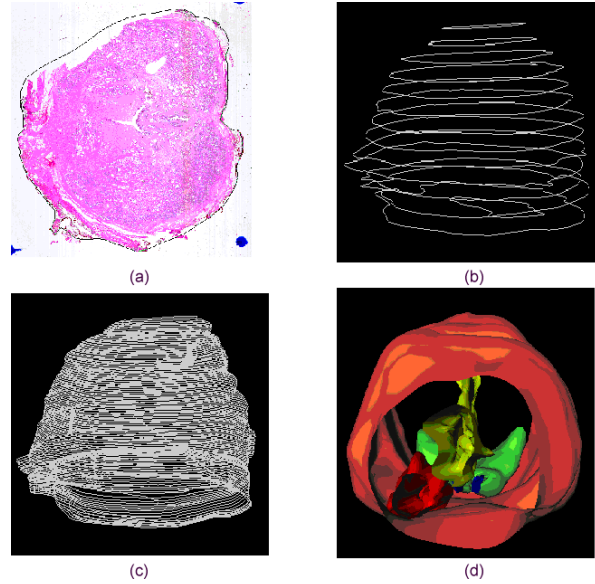


Figure 1: Figure 1: 3-D reconstruction of prostate models: (a) Digitized image of a single slice of a sectioned prostate(b) Stacked surgical margin contour controls of original slices. (c) Surgical margin contour interpolation (d) Final 3-D reconstructed prostate model.

of a 3-D visualization system for simulation of prostate biopsies. This system enables a surgeon to conduct a virtual needle biopsy. The physician can use a simulated ultrasound probe, get the simulated ultrasound images both in axial and longitudinal directions, position and fire a needle and obtain feedback from each action.

3. Constructing a 3-D Distribution Map of Prostate Cancer

Because of the low resolution of ultrasound, it is not possible for the physician to pinpoint the position of the biopsy needles to a very high degree of accuracy. For this reason, we have divided the prostate into small zones that are still large enough to be identifiable by the physician.

We have thus divided the prostate into a grid of 48 zones, which is likely the the upper limit on the number of zones that can still be accessible by the urologist. The grid has three transverse layers along the (patient's) vertical axis, starting from the base at the lower end, through the mid to the apex at the upper end. Each such layer is divided into four coronal layers from the rear to the front, denoted by posterior 1 (p1), posterior 2 (p2), anterior 1 (a1), and anterior 2 (a2). Finally the layers are divided from left to right into four sagittal layers, denoted by left lateral (ll), left mid (lm), right mid (rm) and right lateral (rl). The 48-zone grid is shown in Figure 2.

In order to investigate the cancer distribution of each zone, the occurrence of cancer was calculated in each of the zones for all 281 patients. A zone is considered positive for a given patient, if it contains any part of a tumor. A special-purpose algorithm was devised [Zeng et al. 2000] to automate the calculation of the distribution map effectively.

A bar chart depicting the cancer distribution in each of the transverse layers is given in Figure 3. The proportion of patients who were found to have cancer in a given zone is

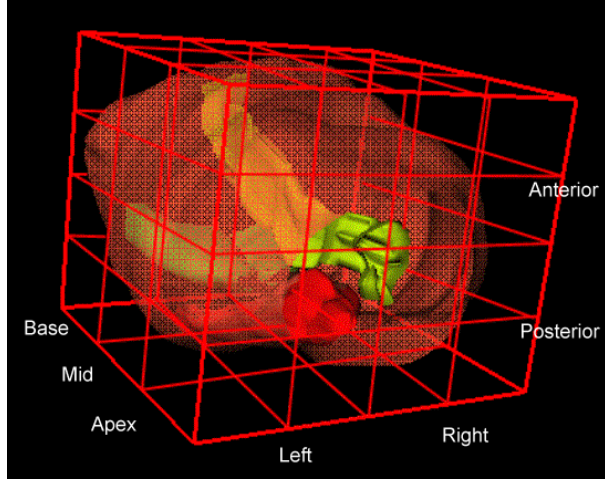


Figure 2: 48-zone grid superimposed over prostate. Grid is slightly exaggerated in size for clarity. Features shown include the urethra, the seminal vesicle, and a tumor in the left posterior apex and mid zones.

presented later, in Table 1. The data shows that cancer is most prevalent in the mid and apex zones, and less prevalent in the base layer. Similarly it is more prevalent in the posterior than in the anterior. There is no substantial difference in tumor distribution between the left and right sides of the tumor.

A key feature of the mapping is that it is invariant to prostate size. Although larger prostates will have larger-sized zones, each zone in different prostate models will have the same spatial meaning.

4. The optimization models

The goal of our research is to determine the zones to be biopsied that maximize the probability of detection of cancer. Diagnosis of cancer will occur if at least one of the needle biopsies is positive (cancerous).

In general the presence of cancer in neighboring zones are statistically dependent events. For this reason, an approach that attempts to calculate the probability that cancer will be present in at least one of j biopsied zones, by calculating the joint probabilities of the relevant underlying events is not likely to be fruitful. A simpler approach is to compute the proportion (or equivalently, the number) of patients whose cancer is indeed detected by the biopsy.

To this end, define the $m \times n$ matrix A by

$$a_{i,j} = \begin{cases} 1 & \text{if patient } i \text{ has cancer in zone } j \\ 0 & \text{otherwise,} \end{cases}$$

where m is the number of prostate models in the study ($m = 281$) and n is the number of zones in the 3-D map ($n=48$). Let

$$x_j = \begin{cases} 1 & \text{if a biopsy is taken in zone } j \\ 0 & \text{otherwise.} \end{cases}$$

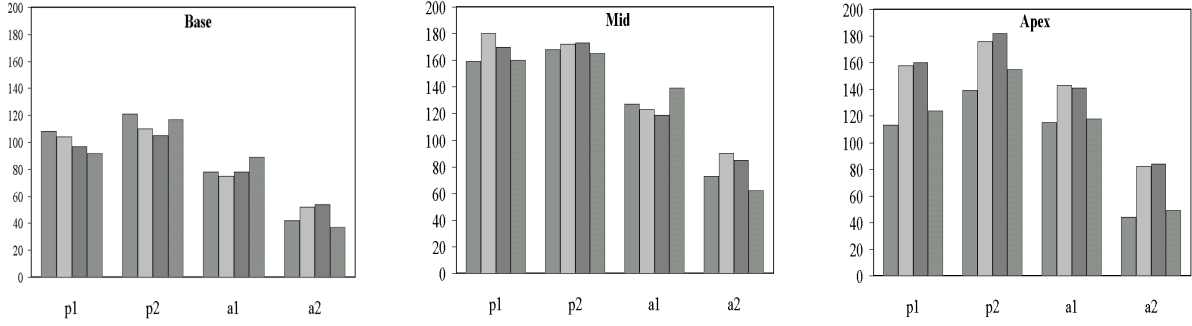


Figure 3: Distribution map of cancer by zone, in base, mid, and apex. Moving from left to right, each block of 4 bars represents zones p1, p2, a1, and a2 respectively, and the bars in each block represent zones ll, lm, rm, and rl respectively

Then the minimum number of zones to be biopsied that would guarantee cancer detection for the entire data set is the solution to the set covering problem

$$\begin{aligned}
 & \text{minimize} && \sum_{j=1}^n x_j \\
 & \text{subject to} && Ax \geq 1 \\
 & && x_j \in \{0, 1\}.
 \end{aligned} \tag{1}$$

It is also possible to determine the biopsy protocol that provides the maximum rate of tumor detection for a given number of needles. Define

$$y_i = \begin{cases} 1 & \text{if test detects cancer in patient } i \\ 0 & \text{otherwise.} \end{cases}$$

Then the maximum number of patients in the data set whose tumor would be detected by a k -zone biopsy can be found by solving the integer program

$$\begin{aligned}
 & \text{maximize} && \sum_{i=1}^n y_i \\
 & \text{subject to} && Ax \geq y \\
 & && \sum_{j=1}^n x_j = k \\
 & && x_j, y_i \in \{0, 1\}
 \end{aligned} \tag{2}$$

Note that the i -th element of Ax gives the number of zones in which cancer is detected for patient i . If this number is zero, then the inequality $Ax \geq y$ forces y_i to be zero. If the number is one or more, the inequality permits y_i to be either 0 or 1, but since the objective is to maximize the sum of the y variables, the optimal solution will have $y_i = 1$.

Two other sets of constraints were incorporated into the models, in some of the runs. The first, imposes left-right symmetry on the biopsied zones ($x_l = x_r$ for every pair of zones

Number of Biopsies	Posterior Only		Posterior + Rear Anterior	
	No. of Patients	Percentage	No. of Patients	Percentage
6	271	96.4%	272	96.8%
8	274	97.5%	280	99.6%
10	275	97.7%	281	100%

Table 1: Number of patients diagnosed by optimal protocol with 6, 8, and 10 needles.

that have left-right symmetry). Physicians prefer left-right symmetry because it simplifies the biopsy procedure, thereby reducing the possibility of probing the wrong zone. Another set of constraints restricts the biopsy to the posterior of the prostate. The reason is that anterior biopsies are more difficult to perform, and more uncomfortable for the patient. We have investigated both protocols restricted to the rear half (posterior) of the prostate and the rear three-fourths (the posterior, plus the rear half of the anterior).

5. Optimal Biopsy Protocols

We used the software package ILOG CPLEX 6.5 to solve the relevant integer programs. In all cases CPLEX solved the problems within seconds, on a variety of platforms.

In solving the set covering problem (1) we found that the minimum number of needle biopsies required to guarantee detection of cancer in all 281 patients is 8. Imposing the left-right symmetry restrictions increases the number of needles required to 10. 10 needles would still cover all patients when the biopsies are restricted to the rear three-fourths. However it is not possible to detect all cancers just by probing the posterior of the prostate. Indeed, in 6 of the 281 patients the cancer was restricted to the anterior of the prostate.

We next determined the maximum number of patients in the data set whose tumor would be detected by a 6-, 8-, and 10-zone (symmetric) biopsy. The results are summarized in Table 1. The corresponding optimal biopsy protocols, however, are not, in every case unique. For example there are two optimal 10-zone protocols in the posterior, both detecting cancer in 275 patients. To assist us further in selecting the protocol, we determined among the optimal solutions the one that maximizes the average number of cancerous zones detected per patient. (We elaborate more on the rationale for this below.) Let K be the maximum number of patients diagnosed in a k -biopsy (for example, $K = 275$ in the case mentioned above). Let e denote an m -vector of ones. Then the (scaled) objective is to maximize

$$e^T A x,$$

subject to the constraints of (2) with the additional constraint $e^T y = K$. Let $s = A^T e$ be the vector whose components give the number of patients in the data set with cancer in each of the zones. Then the objective is to maximize $s^T x$.

The resulting optimal protocols for biopsies in the rear half, and the rear three fourths are shown in Tables 2 and 3 respectively. In both cases the optima are unique. In both cases also, the 6-needle protocol is a subset of the 8-needle-protocol, which in turn is a subset of the 10-needle protocol. Tables 2 and 3 also show the proportion of patients who had cancer in each zone.

The final determination whether to use 6, 8, or 10 needles in the biopsy, and whether to biopsy the rear anterior are beyond the scope of this work. Clearly, the greater the number

lla2 14.9%	lma2 18.5%	rma2 19.2%	rla2 13.2%	lla2 26.0%	lma2 32.0%	rma2 30.2%	rla2 22.1%	lla2 15.7%	lma2 29.2%	rma2 29.9%	rla2 17.4%
lla1 27.8%	lma1 26.6%	rma1 27.8%	rla1 31.7%	lla1 45.2%	lma1 43.8%	rma1 42.4%	rla1 46.3%	lla1 40.9%	lma1 50.9%	rma1 50.2%	rla1 42.0%
llp2 43.1% ***	lmp2 39.1%	rmp2 37.4%	rlp2 41.7% ***	llp2 59.8% ***	lmp2 61.2%	rmp2 61.6%	rlp2 56.7% ***	llp2 49.5% *	lmp2 62.6% ***	rmp2 64.8% ***	rlp2 55.2% *
llp1 38.4%	lmp1 37.0%	rmp1 34.5%	rlp1 32.7%	llp1 56.6%	lmp1 64.1% **	rmp1 60.5% **	rlp1 56.9%	llp1 40.2%	lmp1 56.2%	rmp1 56.9%	rlp1 44.2%
Base				Mid				Apex			

Table 2: Optimal biopsy protocols for 6, 8, and 10 needles, with biopsies restricted to the posterior of the prostate. *** denotes zones that are part of the 6-biopsy protocol; ** denotes the additional zones that are part of the 8-biopsy protocol; * denotes the additional zones that are part of the 10-biopsy protocol

lla2 14.9%	lma2 18.5%	rma2 19.2%	rla2 13.2%	lla2 26.0%	lma2 32.0%	rma2 30.2%	rla2 22.1%	lla2 15.7%	lma2 29.2%	rma2 29.9%	rla2 17.4%
lla1 27.8%	lma1 26.6%	rma1 27.8%	rla1 31.7%	lla1 45.2% ***	lma1 43.8%	rma1 42.4%	rla1 46.3% ***	lla1 40.9%	lma1 50.9% *	rma1 50.2% *	rla1 42.0%
llp2 43.1% **	lmp2 39.1%	rmp2 37.4%	rlp2 41.7% **	llp2 59.8%	lmp2 61.2%	rmp2 61.6%	rlp2 58.7%	llp2 49.5% ***	lmp2 62.6%	rmp2 64.8%	rlp2 55.2% ***
llp1 38.4%	lmp1 37.0%	rmp1 34.5%	rlp1 32.7%	llp1 56.6%	lmp1 64.1% ***	rmp1 60.5% ***	rlp1 56.9%	llp1 40.2%	lmp1 56.2%	rmp1 56.9%	rlp1 44.2%
Base				Mid				Apex			

Table 3: Optimal Biopsy Protocols for 6, 8, and 10 needles, with biopsies restricted to the posterior plus the rear of the anterior. *** denotes zones that are part of the 6-biopsy protocol; ** denotes the additional zones that are part of the 8-biopsy protocol; * denotes the additional zones that are part of the 10-biopsy protocol

of needles, the higher the rate of detection of cancer. But transrectal ultrasound guided needle biopsy of the prostate is a minimally invasive procedure. It is relatively safe, but like all surgical procedures it does carry a small risk for potential morbidity.

With regards to our results, the question remains, what is the statistical validity of the estimated detection rates shown in Table 1. If indeed it were the case, that a needle probe taken in a cancerous zone is always positive, then the confidence intervals for our estimates would be quite narrow. For example, the sample standard deviation for an 8-needle biopsy is (in percentages) 0.86 for posterior only biopsies and 0.36 for three fourths biopsies.

Unfortunately it is possible that a biopsy in a cancerous zone will be negative. Indeed, in creating the map, for a given patient a given zone was deemed cancerous even if it had a small cancerous part.

Estimating the probability that the needle biopsy core will be positive given that the zone is cancerous is a complex problem. It is difficult because cancerous cells are not distributed randomly within a zone; furthermore, because of the contiguous nature of core, the cells biopsied are not statistically independent. If we assume however, that this probability is equal for all zones, then for each patient the best strategy would maximize number of cancerous zones covered. It is for this reason, that we have chosen among the multiple optimal solutions to (2) the one that maximizes the average number of cancerous zones detected per patient.

6. Conclusions

In the past, prostate cancer biopsy protocols were based on long term experiences of the physicians, and were evaluated by their empirical detection rate. We believe that our work is the first to develop a 3-D statistical distribution map of prostate cancer based on real prostate specimens, and the first to use this map to optimize prostate cancer biopsy protocols. We have proposed biopsy protocols that could potentially improve significantly the detection rate of prostate cancer.

We are currently conducting a more comprehensive study of biopsy protocols, based on the patients age, race (prostate cancer has a higher prevalence among African Americans) and PSA level. In parallel, we are utilizing the cancer distribution map and the optimized biopsy protocols to develop an image-guided *in vivo* online system that will assist the urologist in the biopsy.

Acknowledgements

Ariela Sofer is partially supported by National Science Foundation grant DMI-9800544. Jianchao Zeng is supported in part by The US Army Medical Research and Materiel Command, The Whitaker Foundation Biomedical Engineering Program and the Center for Prostate Disease Research. We wish to acknowledge the input of Xiaohu Yao, Wei Zhang, Isabell A. Sesterhenn, and Judd W. Moul.

References

American Cancer Society web page - <http://www.cancer.org/statistics/>

Bankhead C. 1997, "Sextant biopsy helps in prognosis of Pca, but its not foolproof," *UROLOGY TIMES* Vol. 25, No. 8. (August).

- Bauer, J.J., J. Zeng, J. Weir, W. Zhang, I.A. Sesterhenn, R. R. Connelly, S. K. Mun and J. Moul, 1999, "Three-dimensional computer-simulated prostate models: lateral prostate biopsies increase the detection rate of prostate cancer," *UROLOGY*, Vol. 53, pp. 961–967.
- Chang J.J., K. Shinohara, V. Bhargava, J.C.Presti Jr. 1997, "Prospective evaluation of lateral biopsies of the peripheral zone for prostate cancer detection," *J. UROLOGY*, Vol. 160, pp. 2111–2114.
- A.L. Eskew, R.L. Bare, D.L. McCullough. 1997, "Systematic 5-region prostate biopsy is superior to sextant method for detecting carcinoma of the prostate." *J. UROLOGY*, Vol. 157, pp. 199–202.
- Hodge K.K, J.E.McNeal, M.K. Terris, and T.A. Stamey. 1989, "Random systematic versus directed ultrasound guided trans-rectal core biopsies of the prostate," *J. UROLOGY* Vol. 142, pp. 71–74
- ILOG CPLEX 6.5 User Manual, ILOG, 1999.
- Nemhauser G, and L. Wolsey. 1988, "INTEGER AND COMBINATORIAL OPTIMIZATION," Wiley.
- O'Dowd, G.J, M.C. Miller, R. Orozco and R.W. Veltri. 2000, "Analysis of repeated biopsy results within 1 year after a noncancer diagnosis," *UROLOGY*, Vol 55, No. 4, pp.553-558.
- Rabbani F., N. Stroumbakis, B.R. Kava, M.S. Cookson, W.R. Fair. 1998, "Incidence and clinical significance of false-negative sextant prostate biopsies," *J. UROLOGY* Vol. 159, pp. 1247–1250.
- Zeng J., C. Kaplan, J. Xuan, I.A. Sesterhenn, J.H. Lynch, M.T. Freedman and S.K. Mun, 1998a. "Optimizing prostate needle biopsy through 3-D simulation", SPIE Medical Imaging Conference, San Diego. pp. 488-496.
- Zeng, J., C. Kaplan, J.J. Bauer, I. Sesterhenn, J. Moul and S. K. Mun, 1998b, "Visualization and evaluation of prostate needle biopsy. *Proc. of The First International Conference on Medical Image Computing and Computer-Assisted Intervention.*
- Zeng, J., J.J. Bauer, X. Yao, W. Zhang, I.A. Sesterhenn, R.R. Connelly, J. Moul and S. K. Mun, 2000, "Building an accurate 3D map of prostate cancer using computerized models of 280 whole-mounted radical prostatectomy specimens . Presented at *SPIE Medical Imaging Conference.*